Antiferromagnetic resonance in MnF_2 over wide ranges of frequency and magnetic field

1996 J. Phys.: Condens. Matter 8 7349

(http://iopscience.iop.org/0953-8984/8/39/011)

J. Phys.: Condens. Matter **8** (1996) 7349–7354. Printed in the UK

Antiferromagnetic resonance in MnF_2 over wide ranges of frequency and magnetic field

M Hagiwara†, K Katsumata†, I Yamada‡ and H Suzuki§

† The Institute of Physical and Chemical Research (RIKEN), Wako, Saitama 351-01, Japan
‡ Department of Physics, Faculty of Science, Chiba University, Yayoi-cho, Inage-ku, Chiba 263, Japan
§ Keycom Company Limited, Tokorozawa, Saitama 359, Japan

Received 14 May 1996

Abstract. Antiferromagnetic resonance (AFMR) experiments on a well characterized single-crystal sample of MnF_2 have been performed using a spectrometer with wide ranges of both frequency and magnetic field. All the AFMR modes predicted from the theory have been observed. We find a significant contribution of the non-linear term in the expression of the AFMR frequency to the temperature dependence of the resonance point in the high-field low-frequency region.

1. Introduction

Manganous fluoride (MnF_2) has been studied extensively as a prototypical example of antiferromagnets with uniaxial anisotropy (Landolt–Börnstein 1994). There has been a number of experiments performed on this compound, including magnetization (Jacobs 1961), neutron scattering (Erickson 1953) and nuclear magnetic resonance (NMR) (Shulman and Jaccarino 1957, Heller and Benedek 1962) measurements. From antiferromagnetic resonance (AFMR) measurements (Foner 1957, Johnson and Nethercot 1959), information about the exchange and anisotropy energies has been obtained with the help of theory (Nagamiya 1951, Keffer and Kittel 1952). In the 1950s, the frequency of electron spin resonance (ESR) apparatus was limited to ∼100 GHz and the steady magnetic field to ∼1 T. Therefore, in the early AFMR experiments on MnF_2, the measurements were performed at low frequencies with pulsed magnetic fields (Foner 1957) or at low fields with frequency multipliers (Johnson and Nethercot 1959). It is now possible to have centimetre, millimetre and submillimetre waves ranging from ∼1 GHz to ∼600 GHz using e.g. klystrons, Gunn oscillators, Carcinotrons (the trademark name for backward-wave oscillators of Thomson Co.) and a millimetre vector network analyzer, and up to ∼7 THz using a far-infrared laser. Stable high magnetic fields up to 20 T are now available with a superconducting magnet.

In the Institute of Physical and Chemical Research (RIKEN), we are building an ESR spectrometer with wide frequency and field ranges. In a previous paper (Hagiwara *et al* 1994), we reported the results of AFMR measurements on Rb_2MnCl_4, a quasi-two-dimensional antiferromagnet, obtained with the apparatus. We have observed all the AFMR modes predicted by the theory (Nagamiya 1951, Keffer and Kittel 1952) except for the critical field resonance. In the present study, we have tried to measure AFMR of MnF_2 and have been successful in observing all of the AFMR modes expected from the theory.

0953-8984/96/397349+06$19.50

Moreover, we have found a significant contribution of the non-linear term in the expression of the AFMR frequency to the temperature dependence of the resonance point in the high-field low-frequency region.

The format of this paper is as follows. In section 2 we describe the crystal and magnetic structures of MnF_2. Experimental details are given in section 3. In section 4 we present results of the AFMR experiments and their analysis.

2. Crystal and magnetic structures of MnF_2

The crystal structure of MnF_2 belongs to the tetragonal space group D_{4h}^{14} with two molecules per unit cell. The lattice constants at room temperature are $a = 4.8734$ Å and $c = 3.3103$ Å (Griffel and Stout 1950).

From the neutron scattering study of Erickson (1953) below the Néel temperature ($T_N = 67.34$ K) (Heller and Benedek 1962), the magnetic structure of MnF_2 was determined. In the ordered phase, the spins at body centre sites point antiparallel to those at the corner sites with the spin easy axis parallel to the c axis. The main origin of the magnetic anisotropy is the dipole–dipole interaction.

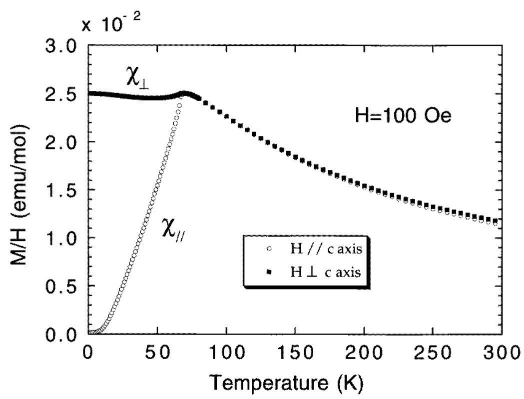

Figure 1. The temperature dependence of the molar magnetic susceptibilities parallel and perpendicular to the c axis of MnF_2 measured at 100 Oe.

3. Experimental details

3.1. Sample preparation and characterization

Single crystals of MnF_2 were grown by the Bridgman method. A commercially available powder of MnF_2 with 4 N purity was placed in a Pt crucible, melted at about 900 °C and cooled at the rate of 1°C h^{-1} under an atmosphere of mixed N_2 and HF gas. A transparent pink coloured single crystal was obtained. A thin disc of MnF_2 with the c axis perpendicular to the plane was cut from a larger crystal.

In order to characterize the crystal, we have measured the temperature dependence of the magnetization (M) under an external magnetic field (H) using a SQUID magnetometer (Quantum Design's MPMS2). The results are shown in figure 1. There is no anisotropy in the susceptibility (M/H) along the c axis ($\chi_\parallel$) and c plane ($\chi_\perp$) above about 67 K. On the other hand, $\chi_\parallel$ and $\chi_\perp$ behave quite differently below ~67 K, which is a typical behaviour below T_N in an antiferromagnet with uniaxial anisotropy. The present results of the susceptibility are consistent with those reported before (Trapp and Stout 1963).

3.2. ESR measurements

The ESR spectrometre consists of two main parts (a magnet and a microwave source) and measuring instruments. The microwaves are generated from three klystrons covering the frequency ranges 20, 50 and 90 GHz, respectively, one Gunn oscillator with the frequency range of 35 GHz and two Carcinotrons operating one at 200 GHz and one at 300 GHz. The magnetic field is produced by a superconducting magnet produced by Oxford Instruments, UK. The magnetic field can be swept up to 18 T at 4.2 K and up to 20 T at 2.2 K. A Dewar (variable-temperature insert) is used to change the temperature of the sample space from 1.6 to 200 K. At the lower frequencies, conventional cryostats with resonant cavities are used. At the higher frequencies, a special wave guide with a dielectric material inside was used to minimize the transmission loss. At 300 GHz, the loss of this waveguide (5 dB m^{-1}) is about 20 times smaller than that of a stainless steel pipe without the dielectric material (18 dB m^{-1}). The temperature of the sample is measured by a calibrated carbon glass thermometer placed close to it. The ESR measurement is fully automated by the use of a computer (Hewlett–Packard 9000-360CH).

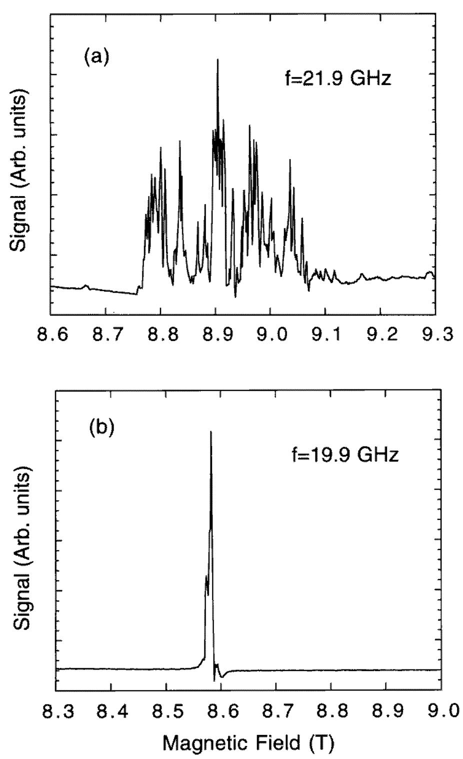

Figure 2. (a) An example of the ESR signal of an as-grown crystal of MnF_2obtained at 21.9 GHz. (b) An example of the ESR signal of single-crystal MnF_2 obtained at 19.9 GHz after the sample had been annealed and etched.

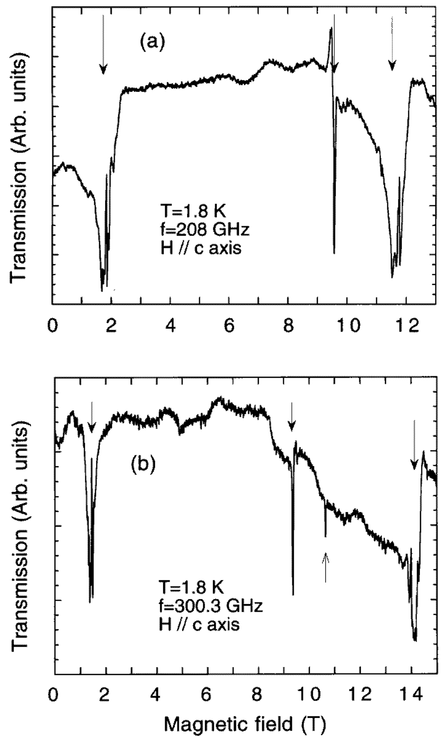

Figure 3. Typical examples of ESR signals obtained at 1.8 K for the frequencies of (a) 208 GHz and (b) 300.3 GHz when the external magnetic field is applied to the *c* axis. Thick arrows show the AFMR signal positions and the thin arrow shows the paramagnetic resonance position probably due to free Mn^{2+}.

4. Experimental results and analysis

We show in figure 2(a) an example of the ESR signal at 21.9 GHz in an as-grown crystal of MnF_2 when the external magnetic field is applied along the *c* axis. We see many ESR lines over the wide field range of about 0.3 T. Figure 2(b) shows the ESR signal after the sample has been annealed at a temperature just below the melting temperature followed by etching with a solution of NH_4F. In this way, we were able to get a sharp AFMR signal. The full width at half maximum is about 0.01 T, which is comparable with that reported before (Kotthaus and Jaccarino 1972). The small structure in figure 2(b) may originate from magnetostatic modes, because the splitting between the magnetostatic modes and the uniform mode is about 0.01 T, which is close to the value (0.03 T) estimated for a disc shaped sample (Gordon *et al* 1965, Beeman 1966).

In figures 3(a) and (b) are shown typical examples of ESR signals along the *c* axis obtained at 1.8 K for the frequencies of 208 and 300.3 GHz, respectively. We take one of the strongest signals as the resonance field when several lines are present.

Figure 4 summarizes all the AFMR data obtained at 1.8 K in the frequency (ν)–magnetic field (H) plane. It is immediately clear that MnF_2 shows the expected AFMR modes typical of a uniaxial antiferromagnet.

We have measured the temperature dependence of the resonance field in one of the AFMR modes at fixed frequencies as shown in figure 5. All of the resonance fields at 21.7,

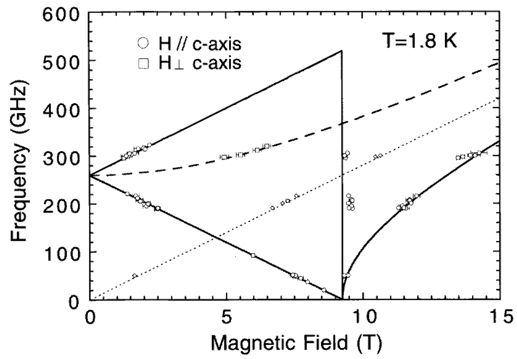

Figure 4. Frequency versus external magnetic field relations of the AFMR signals in MnF_2. The full straight lines, the full curve and the broken curve are the theoretical ones discussed in the text. The dotted line is the paramagnetic resonance line with $g = 2.00$.

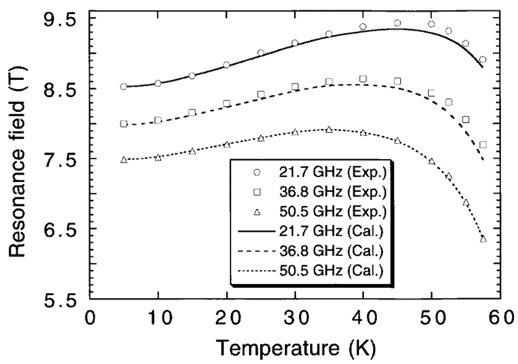

Figure 5. The temperature dependence of the AFMR positions at the designated frequencies. The curves are the theoretical ones discussed in the text.

36.8 and 50.5 GHz have similar behaviour with increasing temperature. Namely, resonance fields increase with increasing temperature and then decrease as the temperature is increased further.

In the following, we analyse the experimental results shown in figures 4 and 5. If the exchange field (H_e) is much larger than the anisotropy field (H_a), the AFMR frequencies of a uniaxial antiferromagnet are given by equations (1)–(3) below (Nagamiya *et al* 1955, Keffer and Kittel 1952, Foner 1963). In MnF_2, $H_e \sim 53$ T and $H_a \sim 0.82$ T so that $H_e \gg H_a$ (Johnson and Nethercot 1959).

$$h\nu/g\mu_B = \sqrt{2K_u/\chi_\perp + (\chi_\parallel H/2\chi_\perp)^2} \pm H(1 - \chi_\parallel/2\chi_\perp) \qquad (H \parallel c, H < H_{SF}) \tag{1}$$

$$h\nu/g\mu_B = \sqrt{H^2 - 2K_u/\chi_\perp} \qquad (H \parallel c, H > H_{SF}) \tag{2}$$

and

$$h\nu/g\mu_B = \sqrt{H^2 + 2K_u/\chi_\perp} \qquad (H \perp c) \tag{3}$$

where h is Planck's constant, g the g-value, μ_B the Bohr magneton, K_u the anisotropy constant and H_{SF} the critical field for spin flop. At low temperatures ($T \ll T_N$), $\chi_\parallel$ is much smaller than $\chi_\perp$, so equation (1) becomes

$$h\nu/g\mu_B = \sqrt{2K_u/\chi_\perp} \pm H. \tag{4}$$

The two full straight lines below 9.3 T in figure 4 represent equation (4), the full curve above 9.3 T equation (2) and the broken line equation (3) with $\sqrt{2K_u/\chi_\perp} = 9.27$ T. This value of the zero-field gap frequency (259.7 GHz) is very close to that reported before (261.4 $\pm$ 1.5 GHz at 0 K) (Johnson and Nethercot 1959). The vertical straight line at 9.27 T represents the critical field resonance mode. We see in figure 4 a good agreement between theory and experiment. In the present experiment we are able to observe all the AFMR modes predicted by the theory.

Next, we analyse the temperature dependence of the resonance field (figure 5). The frequency–field relation of the AFMR mode relevant to the data in figure 5 is given by equation (1) with the minus sign. In this equation, K_u, $\chi_\parallel$ and $\chi_\perp$ depend on temperature. We use for the temperature dependence of the ratio $\chi_\parallel/\chi_\perp$ the experimental value deduced from figure 1. The g-value is obtained from figure 4 to be 2.00. Then, we have only one adjustable parameter, $K_u/\chi_\perp$. We obtain the temperature dependence of $K_u/\chi_\perp$ by fitting equation (1) with the data taken at 50.5 GHz. We can then compare the theory with the experiments performed at 21.7 and 36.8 GHz without any adjustable parameter. The agreement between the theory and the experiment at both frequencies is satisfactory. The broad peak in the temperature dependence of the resonance fields originates from the combined effect of the two terms, $2K_u/\chi_\perp$ and $(\chi_\parallel H/2\chi_\perp)^2$ in equation (1). The same behaviour has been observed in Rb_2MnCl_4 (Hagiwara *et al* 1994).

In conclusion, we have made ESR measurements on a well characterized single crystal of MnF_2 using a wide-frequency and high-field spectrometre installed in RIKEN. We have been successful in observing all the AFMR modes expected for an antiferromagnet with uniaxial anisotropy. We have also observed the effect of the non-linear term on the temperature dependence of the AFMR position. All these experimental results agree quantitatively with the theory.

Acknowledgments

This work was supported by the MR Science Research Programme of RIKEN.

References

Beeman D E 1966 *J. Appl. Phys.* **37** 1136–7
Erickson R A 1953 *Phys. Rev.* **90** 779–85
Foner S 1957 *Phys. Rev.* **107** 683–5
——1963 *Magnetism* vol 1, ed G T Rado and H Suhl (New York: Academic) pp 383–447
Gordon N I, Kadigrobov M and Savchenko M A 1965 *Sov. Phys.–JETP* **21** 576–9
Griffel M and Stout J W 1950 *J. Am. Chem. Soc.* **72** 4351–3
Hagiwara M, Katsumata K and Tuchendler J 1994 *J. Phys.: Condens. Matter* **6** 545–50
Heller P and Benedek G B 1962 *Phys. Rev. Lett.* **8** 428–32
Jacobs I S 1961 *J. Appl. Phys.* **32** 61s-62s
Johnson F M and Nethercot A H Jr 1959 *Phys. Rev.* **114** 705–16
Keffer F and Kittel C 1952 *Phys. Rev.* **85** 329–37
Kotthaus J P and Jaccarino V 1972 *Phys. Rev. Lett.* **28** 1649–52
Landolt–Bornstein 1994 New Series Group III, vol 27j1, (Berlin: Springer) pp 1–135 and references therein
Nagamiya T 1951 *Prog. Theor. Phys.* **6** 342–55
Nagamiya T, Yosida K and Kubo R 1955 *Adv. Phys.* **4** 1–112
Shulman R G and Jaccarino V 1957 *Phys. Rev.* **108** 1219–31
Trapp C and Stout J W 1963 *Phys. Rev. Lett.* **10** 157–9